JOURNAL OF GUIDANCE, CONTROL, AND DYNAMICS
Vol. 29, No. 4, July–August 2006

Engineering Notes

ENGINEERING NOTES are short manuscripts describing new developments or important results of a preliminary nature. These Notes should not exceed 2500 words (where a figure or table counts as 200 words). Following informal review by the Editors, they may be published within a few months of the date of receipt. Style requirements are the same as for regular contributions (see inside back cover).

Indirect Optimization of Low-Thrust Capture Trajectories

Marco La Mantia* and Lorenzo Casalino†
Politecnico di Torino, 10129 Torino, Italy

DOI: 10.2514/1.18986

Introduction

ELECTRIC propulsion (EP) has proven to be a viable option for the exploration of the solar system because of the low propellant consumption. Even when EP is used for an interplanetary flight, chemical propulsion (CP) is usually employed to leave the Earth, as in the case of the Deep Space 1 mission [1] and the upcoming DAWN mission.‡ EP has been proposed to perform the capture at Mars on arrival for a sample return mission [2].

The benefit of using the same high-specific-impulse EP system to perform different mission legs is obvious, at least when a longer trip time can be tolerated. In this note, the Earth-capture of a spacecraft that returns from an interplanetary mission is optimized by means of a numerical procedure, which is based on the optimal control theory (OCT). The results can easily be extended to trajectories around other planets and escape maneuvers. The two-body problem formulation is adopted for a preliminary analysis of this mission and only the return maneuver inside the Earth's gravity field is considered.

The strategies that minimize the total propellant mass required for the low-thrust transfer from the edge of the terrestrial sphere of influence to the desired low Earth orbit (LEO) are sought when the approach velocity is assigned. The trajectories are split into two parts. The *approach* phase, which can also involve ballistic arcs, is numerically optimized and inserts the spacecraft into a high circular orbit. The *spiral* phase brings the probe to the final LEO and is analyzed by adopting Edelbaum's approximation [3] (i.e., an almost circular trajectory is considered). The junction point between these parts is also optimized. A comparison with the results of a recent note [4], where Kluever presented a similar approach for the optimization of Earth-capture trajectories, is carried out. The benefit of the proper choice of the offset distance and the utility of coast arcs are shown. The effect of the approach velocity on the performance is also discussed and its maximum value, which allows the capture for given thruster characteristics, is determined.

Presented as Paper 4266 at the 41th AIAA/ASME/SAE/ASEE Joint Propulsion Conference and Exhibit, Tucson, Arizona, 10 July 2005–13 July 2005; received 21 July 2005; revision received 10 December 2005; accepted for publication 15 December 2005.

*Graduate Student, Dipartimento di Energetica, Corso Duca degli Abruzzi, 24, 10129 Torino.

†Associate Professor, Dipartimento di Energetica, Corso Duca degli Abruzzi, 24, 10129 Torino. Senior Member AIAA.

‡Data available on-line at http://dawn.jpl.nasa.gov

Statement of the Problem and Optimization

A spacecraft with a given mass approaches the Earth with known energy. The characteristics of the propulsion system (i.e., thrust and specific impulse) are also known. The spacecraft moves from the boundary of the Earth's sphere of influence to the prescribed final LEO. Only planar trajectories are considered in this note, but the optimization can easily be extended to consider three-dimensional maneuvers, and the same optimization procedure can also be applied to escape trajectories [5].

The capture maneuver is split between the approach and spiral phases; the numerical integration only regards the approach phase and starts at the boundary of the terrestrial sphere of influence (subscript 0), which is conventionally fixed at 1,000,000 km, and is stopped at the beginning of Edelbaum's spiral (subscript f). The spacecraft position $\boldsymbol{r}$ is expressed with polar coordinates r and ϑ; the reference axis $\vartheta = 0$ is opposite the approach velocity $\boldsymbol{V}_0$. The velocity vector $\boldsymbol{V}$ is described by the radial component u and the tangential component v. The spacecraft mass completes the set of state variables. The state equations are

$$\frac{\mathrm{d}\boldsymbol{r}}{\mathrm{d}t} = \boldsymbol{V} \qquad \frac{\mathrm{d}\boldsymbol{V}}{\mathrm{d}t} = \boldsymbol{g} + \frac{\boldsymbol{T}}{m} \qquad \frac{\mathrm{d}m}{\mathrm{d}t} = -\frac{T}{c} \tag{1}$$

where $\boldsymbol{T}$ is the engine thrust and $\boldsymbol{g}$ is the gravitational acceleration (an inverse-square gravity field is assumed throughout); the propellant mass-flow rate is expressed by the ratio of the thrust magnitude to the exhaust velocity c. All variables are made nondimensional to improve the integration accuracy; an appropriate radius ($r_{\mathrm{ref}} = 250,000$ km), the corresponding circular velocity ($V_{\mathrm{ref}} = 1.2627$ km/s) and the spacecraft initial mass m_{ref} are assumed as reference values.

The magnitude of the initial velocity V_0 is assigned; the offset distance and the entry flight path angle are unknown and optimized; this is acceptable when the dimension of the sphere of influence is negligible with respect to the heliocentric distances, as in the case of Earth-Mars trajectories. The initial velocity components are therefore related to the entry point position, as shown in Fig. 1: the entry anomaly dictates the flight path angle $\gamma_0 = \tan^{-1}(u_0/v_0)$, as $\vartheta_0 - \gamma_0 = 90$ deg. The constraining boundary conditions are $r_0 = 4$, $u_0 = -V_0 \cos\vartheta_0$, $v_0 = V_0 \sin\vartheta_0$, and $m_0 = 1$ at the entry point, and $u_f = 0$ and $v_f^2 - 1/r_f = 0$ at the spiral injection. The spacecraft mass at the arrival orbit (subscript LEO) is maximized

$$\Phi = m_{\mathrm{LEO}} = m_f \exp(-\Delta V_S/c) \tag{2}$$

where ΔV_S is the velocity variation that is required for Edelbaum's spiral [3]; for the planar case $\Delta V_S = v_{\mathrm{LEO}} - v_f$, where v_{LEO} is the circular velocity at the LEO radius.

The indirect optimization method [6], which has been widely applied for orbital mechanics problems at the Politecnico di Torino (Italy), is based on OCT. An adjoint variable is associated to each state equation and the Hamiltonian function is introduced:

$$H = \boldsymbol{\lambda}_r^T \boldsymbol{V} + \boldsymbol{\lambda}_V^T (\boldsymbol{g} + \boldsymbol{T}/m) - \lambda_m T/c \tag{3}$$

The Euler–Lagrange equations for the adjoint variables are derived [7]

$$\left[\frac{\mathrm{d}\boldsymbol{\lambda}_r}{\mathrm{d}t}\right]^T = -\boldsymbol{\lambda}_V^T \left[\frac{\partial \boldsymbol{g}}{\partial \boldsymbol{r}}\right] \qquad \left[\frac{\mathrm{d}\boldsymbol{\lambda}_V}{\mathrm{d}t}\right]^T = -\boldsymbol{\lambda}_r^T \qquad \frac{\mathrm{d}\lambda_m}{\mathrm{d}t} = \frac{\lambda_V T}{m^2} \tag{4}$$

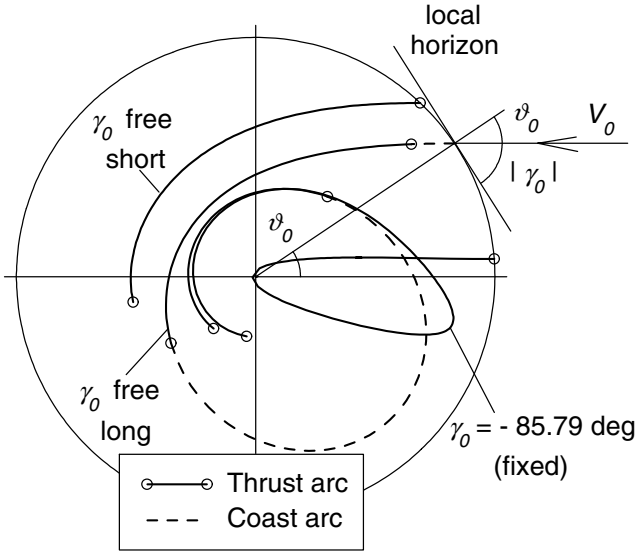

Fig. 1 Approach phase of capture trajectories.

where the gravity-gradient matrix is introduced. Equations (1) and (4) constitute the system of differential equations, which is solved numerically.

Continuous thrust capability without Earth-shadow effects is assumed. The thrust direction and its magnitude are considered as control variables; these must maximize H in agreement with Pontryagin's maximum principle (PMP) [7]. The optimal thrust direction is parallel to the velocity adjoint vector $\boldsymbol{\lambda}_V$, which is usually called the primer vector [8]. The *switching function*

$$S_F = \frac{\lambda_V}{m} - \frac{\lambda_m}{c} \tag{5}$$

is introduced, and Eq. (3) is rewritten as

$$H = \boldsymbol{\lambda}_r^T \boldsymbol{V} + \boldsymbol{\lambda}_V^T \boldsymbol{g} + T S_F \tag{6}$$

The thrust magnitude assumes its maximum value when the switching function S_F is positive (thrusting arcs), whereas it is set to zero when S_F is negative (coast arcs), to maximize the Hamiltonian. The succession of arcs, that is, the trajectory switching structure, is assigned a priori, and the arc lengths are additional unknowns. The optimization procedure provides a solution which is then checked in the light of PMP, by means of an analysis of the switching function; if PMP is violated, coast or thrust arcs are inserted or removed, in accordance with the switching function behavior, to obtain an improved solution (e.g., a coast arc is introduced when S_F becomes negative during a thrust arc).

The boundary conditions for optimality are provided by OCT [6,7] to complete the differential system and define a multipoint boundary value problem. Some of the variable initial values and constant parameters (e.g., the arc lengths) are unknown, and are determined by means of a procedure [9] based on Newton's method. Tentative values are assumed for the unknowns and progressively modified to fulfill the boundary conditions (both constraining equations and conditions for optimality), which are posed in nondimensional form. During each iteration the errors on the boundary conditions and the error-gradient matrix are numerically evaluated; the unknowns are corrected to nullify the errors with the assumption of linear behavior. The optimization procedure showed good robustness and no major difficulties were encountered in the attempt to obtain converged solutions with a 10^{-10} tolerance on the boundary conditions. For each choice of the initial conditions (e.g., spacecraft initial mass, thrust, approach velocity) an all-propulsive trajectory can first be computed; convergence is easily obtained because of the limited number of unknowns (an initial guess may also be derived from previous solutions for different parameters). The switching function is then analyzed and coast arcs are introduced in correspondence of negative S_F values. The all-propulsive solution with the addition of short coast arcs where S_F has peak negative values can be used as initial guess to obtain convergence to the optimal solution, which satisfies PMP.

Results

Diverse boundary conditions and a different approximation of the spiral phase have been assumed in a recent note by Kluever [4], who presented a three-dimensional, all-propulsive capture trajectory. In his note, Kluever assigns the direction of V_0 by means of the initial flight path angle $\gamma_0 = -85.79$ deg; in the present note the initial flight path angle remains open to show the benefit of choosing the offset distance properly. Kluever uses Perkins's approximation [10], which is based on a constant acceleration trajectory with thrust parallel to the velocity, for the spiral, whereas Edelbaum's approximation is here adopted. Both trajectories are suboptimal as they constrain the flight path angle at the spiral start, but Edelbaum's approximation is preferable for two main reasons. First, the capture maneuver that uses Edelbaum's spiral provides better performance than the one which employs Perkins's spiral (see Table 1), and therefore offers a better estimation of the actual optimum. Second, Edelbaum's approximation allows an accurate treatment of the three-dimensional problem and the optimization procedure can easily find the optimal partition of the plane change between the approach and spiral phases [5] (Perkins's spiral does not account for plane change). Moreover, no curve fits or other approximations are required.

An all-propulsive trajectory, similar to that proposed by Kluever, is first considered, but a planar case is assumed. The relevant data are $V_0 = 0.8562$ (1.0811 km/s), $T = 0.0545$ (0.1094 N for a 315 kg initial mass), $c = 30$ (roughly corresponding to a 3860 s specific impulse). The radius of the low circular orbit, which is chosen as the arrival orbit, is $r_{\mathrm{LEO}} = 0.028$ (7000 km). These data are adopted throughout, unless otherwise specified.

Trajectories with constrained initial flight path angles are first considered and $\vartheta_0 = 4.21$ deg ($\gamma_0 = -85.79$ deg) is added to the constraining equations. The results are presented in Table 1 and the approach phase is shown in Fig. 1: the spacecraft moves close to the Earth and reaches a very low perigee, and then inserts itself into a higher orbit, where the spiral starts. Similar results are obtained when Perkins's approximation is used for the spiral, as, in this case, the flight path angle at the spiral insertion γ_f is close to 0 (the details of the optimization are not given here). The performance is marginally better when Edelbaum's approximation is used, possibly because of the lower gravity losses, as the flight path angle is, on average, closer to zero. Neither trajectory is optimal: S_F becomes negative during the approach phase, thus suggesting the introduction of coast arcs. This can be explained by considering that the thrust is not used efficiently; because of the radial entry, the spacecraft, which is first braked

Table 1 Characteristics and performance of planar capture trajectories

Approach type	Spiral type	γ_0, deg	r_f, 10^3 km	γ_f, deg	m_f	m_{LEO}	τ_A, days	τ_S, days	τ, days
γ_0 fixed	Edelbaum	−85.8	253	0	0.962	0.815	47.9	185.6	233.5
γ_0 fixed	Perkins	−85.8	234	−3.4	0.960	0.814	50.4	184.5	234.9
γ_0 free-short	Edelbaum	−43.5	523	0	0.985	0.826	18.7	200.7	219.4
γ_0 free-short	Perkins	−46.3	378	−11.5	0.977	0.822	28.7	195.9	224.6
γ_0 free-long	Edelbaum	−56.2	280	0	0.981	0.829	65.3	191.0	256.3
γ_0 free-long	Perkins	−54.8	248	−4.0	0.978	0.828	61.4	188.8	250.3

during the perigee passage (to perform the capture), must then be accelerated during the apogee passage (to make the orbit circular, or almost circular, for the insertion into the spiral). The acceleration increases the spacecraft energy and makes these trajectories less efficient.

When γ_0 is open two improved trajectories are obtained (see Fig. 1 and Table 1). In the *short* solution the spacecraft directly enters the spiral during the first revolution; the switching function is always positive and the approach phase consists of a single braking burn (the angle between the velocity and thrust vectors is always close to 180 deg), which reduces the energy until a high circular orbit is obtained. The spacecraft does not pass close to the Earth. Both the trip time and propellant consumption are reduced in comparison to the trajectory with $\gamma_0 = -85.79$ deg; the propellant consumption shows a 6% decrease. The use of Perkins's spiral produces quite different results; a negative flight path angle is required at the injection, but the braking that can be obtained during the descent phase is limited, and the approach phase must be lengthened to rotate the velocity toward the Earth, resulting in additional losses.

The optimization procedure also yields a *long* trajectory, which enters the spiral during the second revolution. The switching structure has been modified by adding two coast arcs, as a four-arc structure is found to be optimal in the light of PMP: The engine thrusts inside the sphere of influence after a short coast arc, to perform a first braking at the perigee passage. The engine is turned off during apogee passage and thrusts again to perform a second braking maneuver for the insertion into the spiral (the coast arc is symmetrically centered around the apogee). An additional 1.5% reduction of the propellant consumption is obtained, as the portion of trajectory that is approximated by Edelbaum's spiral is reduced in favor of the optimized approach phase; two perigee burns replace the single burn of the short trajectory, thus reducing the velocity losses related to the low-thrust level and improving the LEO mass, as the braking is conveniently performed at low radius. The benefit, in terms of propellant consumption, is limited, whereas the introduction of coast arcs increases the trip time. Only marginal improvements can be obtained by lengthening the approach phase any further (trajectories with the insertion into the spiral at the third revolution or even later have also been analyzed), with a resulting intolerable increase in the trip time. Note that the global optimum would require an infinite number of revolutions and an infinite trip time. Infinitesimal thrust arcs should be performed during each revolution in correspondence to the most favorable positions (i.e., apogee and perigee) to avoid gravitational and misalignment losses, which are typical of EP.

The direct insertion into the desired LEO with CP requires $\Delta V = 3.22$ km/s; if a 386 s specific impulse is assumed ($c = 3$), the nondimensional LEO mass becomes 0.428, which can be considered to be the mission payload (the mass of the CP system is usually negligible). This value should be compared with the LEO mass of EP trajectories when the spacecraft already has an EP system, which has been used for the interplanetary leg, on board; EP allows a 93% payload increase. When the capture mission is considered separately and requires a dedicated propulsion system, its mass, which is usually considered to be proportional to the electric power (and to the thrust power $Tc/2$ when constant thrust efficiency is assumed), penalizes the payload $m_u = m_{\mathrm{LEO}} - \beta Tc/2$. If $\beta = 0.4$ is assumed for the specific mass of the propulsion system (i.e., roughly 50 kg/kW, consistent with current solar electric propulsion [2]), the benefit of EP is reduced to 17%, but it can be improved by optimizing the specific impulse [5], i.e., c. Remember that the trip time is remarkably lower when CP is used (only 7.7 days, in this case).

The initial velocity V_0 has a large influence on the mission characteristics for a given thruster performance, as it determines the amount of energy that needs to be dissipated to perform the capture. The effect of V_0 on the performance is shown in Fig. 2. A limiting value V_0^* exists; for larger velocities, the spacecraft exits the sphere of influence and the capture cannot be performed. A simple optimization problem is defined to evaluate V_0^* for given a T and c. The same boundary conditions as those of the previous section are posed at point 0, but $V_0^2 = u_0^2 + v_0^2$ is now left free and maximized. At the final point, v_f is left free (insertion into the spiral is not required) and $r_f = 4$ and $u_f = 0$ assure that the spacecraft does not leave the sphere of influence. The boundary conditions for optimality are again derived, and because the final mass is unconstrained, one obtains $\lambda_{mf} = 0$; Eq. (4) states that $\mathrm{d}\lambda_m/\mathrm{d}t > 0$, and λ_m is always negative. Therefore, the switching function is always greater than zero and the thruster is always on.

The maximum approach velocity for $T = 0.1094$ N is $V_0^* = 1.338$ km/s. Both short and long trajectories are modified when V_0 comes close to this value; r_f increases rapidly for the short trajectories, as the energy reduction that can be obtained in a single pass is limited, and the sphere's boundary is reached for $V_0 = 1.31$ km/s. For larger V_0 values, $r_f = 4$ is added to the set of constraints to prevent the exit from the sphere of influence. The LEO mass (Fig. 2) presents a descent as the thrust is not used efficiently, in particular when V_0 is larger than 1.07 km/s. In fact, in these cases, the insertion cannot occur at the perigee of the approach phase because of the greater amount of energy; therefore, the spacecraft travels far from the Earth where the thruster accelerates the spacecraft to perform the insertion at a larger radius, as shown in Fig. 3, which compares the short and long trajectories for $V_0 = 1.325$ km/s (the insertion of the short trajectory occurs at the sphere boundary as $V_0 > 1.31$ km/s). The necessity of first decelerating and then

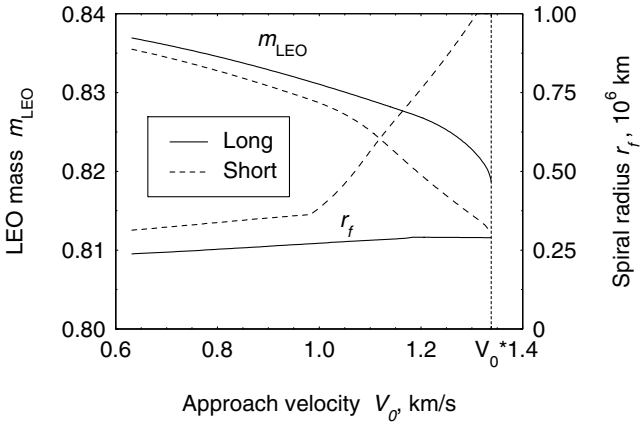

Fig. 2 Influence of the approach velocity for short and long trajectories.

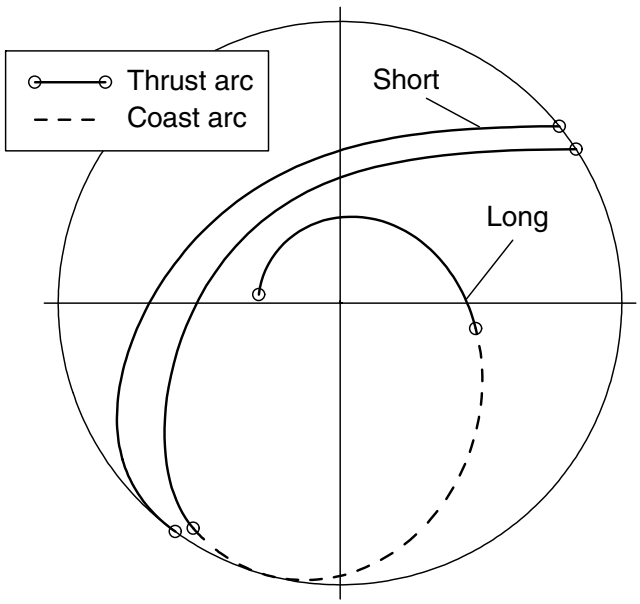

Fig. 3 Short and long capture trajectories for $V_0 = 1.325$ km/s.

accelerating the spacecraft limits the performance of short trajectories and no solution is found for $V_0 > 1.33$ km/s (note that this limiting value is lower than V_0^*).

The LEO mass of the long trajectories decreases less rapidly, as this maneuver is more efficient, at least for $V_0 < 1.17$ km/s, where the initial coast arc vanishes. For larger values, the spacecraft would exit from the sphere of influence after the first perigee passage; therefore, the coast arc is split at the apogee (point a), where $r_a = 4$ and $u_a = 0$ are imposed to prevent the exit from the sphere of influence. The boundary conditions for optimality are again derived. The performance shows a steep decrease as the first thrusting arc is lengthened during the ascent to the apogee (see Fig. 3) and thrust misalignment should be introduced to keep the apogee low. No solution is found above the limiting value V_0^*. The final radius is low, because the insertion into the spiral occurs during the second perigee passage. The more efficient use of thrust, compared with short trajectories, determines the larger final mass.

When V_0 diminishes, the required deceleration becomes less severe and the spacecraft can be inserted into the spiral at a lower radius with a larger LEO mass. The decrease of r_f is more evident for short trajectories, at least when $V_0 \geq 0.99$ km/s; below this value, a coast arc precedes the thrusting phase, and the reduction of the insertion radius becomes less steep. The coast arc length increases as V_0 diminishes, and the same happens for both the coast arcs of the long trajectories.

Conclusions

A numerical procedure for the optimization of Earth-capture trajectories of a spacecraft that employs electric propulsion has been used to find the strategies that minimize the total propellant mass required for the low-thrust transfer from the edge of the terrestrial sphere of influence to the desired low Earth orbit. Edelbaum's approximation was used instead of Perkins's approximation (which has been used in recent literature) to model the suboptimal spiral phase of the trajectory; the comparison shows that a slight performance improvement is obtained by using Edelbaum's spiral. The results also show the benefit of introducing coast arcs during the approach phase and the convenience of choosing the offset distance properly. A simple problem has also been defined to determine the maximum velocity that can allow the capture for a given thrust level. The optimal trajectory is significantly modified when this limit is approached and the performance decrease suggests the use of a larger thrust. The results, which have been obtained assuming the current technological level of solar electric propulsion systems, show that capture trajectories can be performed using off-the-shelf electric engines, with better performance than traditional chemical engines.

References

[1] Rayman, M. D., Varghese, P., Lehman, D. H., and Livesay, L. L., "Results from the Deep Space 1 Technology Validation Mission," *Acta Astronautica*, Vol. 47, Nos. 2–9, 2000, pp. 475–487.

[2] Brophy, J. R., and Rodgers, D. H., "Ion Propulsion for a Mars Sample Return Mission," AIAA Paper 2000-3412, July 2000.

[3] Edelbaum, T. N., "Propulsion Requirements for Controllable Satellites," *ARS Journal*, Vol. 31, No. 8, 1961, pp. 1079–1089.

[4] Kluever, C. A., "Optimal Earth-Capture Trajectories Using Electric Propulsion," *Journal of Guidance, Control, and Dynamics*, Vol. 25, No. 3, 2002, pp. 604–606.

[5] La Mantia, M., and Casalino, L., "Optimization of Low-Thrust Capture and Escape Trajectories," AIAA Paper 2005-4266, July 2005.

[6] Casalino, L., Colasurdo, G., and Pastrone, D., "Optimal Low-Thrust Escape Trajectories Using Gravity Assist," *Journal of Guidance, Control, and Dynamics*, Vol. 22, No. 5, 1999, pp. 637–642.

[7] Bryson, A. E., and Ho, Y. C., *Applied Optimal Control*, Hemisphere, Washington, DC, 1975, pp. 106–108.

[8] Lawden, D. F., *Optimal Trajectories for Space Navigation*, Butterworths, London, 1963, pp. 54–68.

[9] Colasurdo, G., and Pastrone, D., "Indirect Optimization Method for Impulsive Transfer," AIAA Paper 94-3762, Aug. 1994.

[10] Perkins, F. M., "Flight Mechanics of Low-Thrust Spacecraft," *Journal of the Aerospace Sciences*, Vol. 26, No. 5, 1959, pp. 291–297.